

Thermal analysis of lanthanum hydroxide

Ekkehard Füglein · Dirk Walter

CEEC-TAC1 Conference Special Issue
© Akadémiai Kiadó, Budapest, Hungary 2012

Abstract Lanthanum oxide (La_2O_3) is of great interest as catalyst material. When La_2O_3 particles are prepared from lanthanum hydroxide ($\text{La}(\text{OH})_3$) by thermal processes under air, various oxycarbonate phases are formed which are resistant to thermal hydroxylation. This phenomenon has not yet been extensively investigated, even though oxycarbonate phases at the particle surfaces cause a change in lanthanum oxide's catalytic activity. The carbonate phases formed cannot be detected by means of XRD or REM-EDX investigations due to their detection limits. Thermal analysis, particularly TG-FT-IR, allows not only for the detection of the carbonate phases in $\text{La}(\text{OH})_3$, but also for the tracking of the entire dehydration process from $\text{La}(\text{OH})_3$ via LaOOH to La_2O_3 as well as the correct interpretation of mass changes during the thermal transformations. Pursuant to the investigations here carried out, it was determined that carbonate-free lanthanum hydroxide compounds can only be prepared and stored in a CO_2 -free protective gas atmosphere (e.g., argon).

Keywords Lanthanum hydroxide ($\text{La}(\text{OH})_3$) · Carbonate impurities · Thermal transformation · TG-FT-IR

Introduction

Lanthanum oxide (La_2O_3) is being used increasingly as a catalyst material. Special oxidation processes like the flameless methane combustion or graphite oxidation could be realized [1–4]. Furthermore the application of La_2O_3 for the oxidative coupling of methane (OCM) [5, 6] as well as the mechanism of OCM process are well studied and reported [7].

The parameters of particle size and surface morphology, which are important for heterogeneous catalysis, can be optimized by the thermal transformation of lanthanum hydroxide $\text{La}(\text{OH})_3$. The transformation of hexagonal hydroxide ($\text{La}(\text{OH})_3$) to trigonal oxide (La_2O_3) occurs analogously to the hydroxides of aluminum and iron via lanthanum hydroxide oxide (LaOOH) [8].



Due to the fact that it has a larger specific surface than La_2O_3 , lanthanum hydroxide oxide is of special interest as a catalyst material [9, 10].

It is difficult to prepare and characterize lanthanum compounds formed via thermal transformation because of the high CO_2 affinity of the educt $\text{La}(\text{OH})_3$ forming basic carbonates [11]. Investigation of the purity of laboratory- and commercial-quality $\text{La}(\text{OH})_3$ by means of X-ray diffraction (XRD) and scanning electron microscopy (SEM) with energy-dispersive X-ray spectroscopy (EDX) cannot be relied upon to detect carbonate-containing impurities, due to the small particle size and the associated detection threshold. Only by means of coupled thermoanalytical investigations (TG-FT-IR) is it possible to gain insight into the problems surrounding the carbonate formation of $\text{La}(\text{OH})_3$ and the resulting influence on the thermal transformation [12].

E. Füglein
NETZSCH-Gerätebau GmbH, Wittelsbacherstraße
42, 95100 Selb, Germany

D. Walter (✉)
Gefahrstofflaboratorien Chemie und Physik am Institut für
Arbeitsmedizin der Justus-Liebig-Universität,
Aulweg 129, 35392 Giessen, Germany
e-mail: dirk.walter@arbmed.med.uni-giessen.de

Fig. 1 TG-FT-IR results of commercial carbonate-containing $\text{La}(\text{OH})_3$

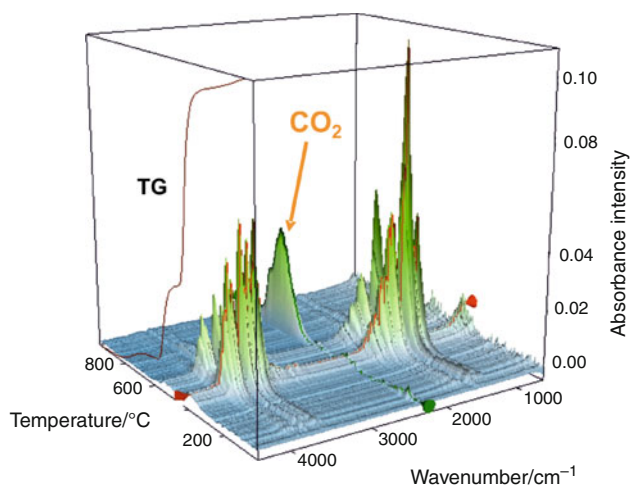
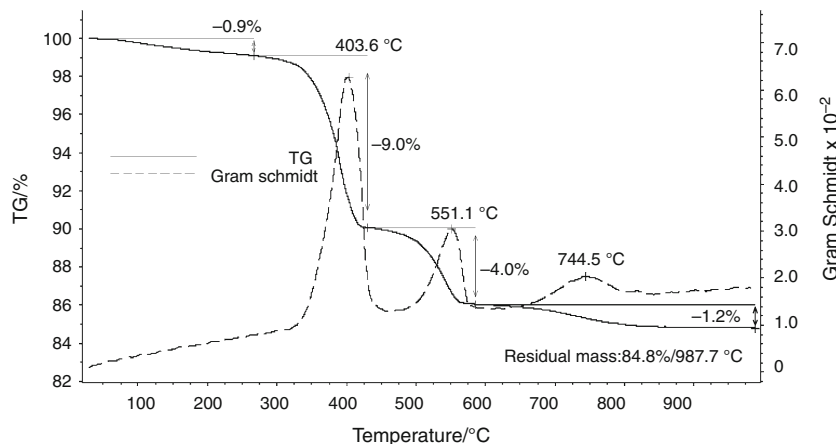


Fig. 2 3-dimensional presentation of all IR spectra from the TG-FT-IR analysis of carbonate-containing $\text{La}(\text{OH})_3$

Experimental

Lanthanum hydroxide (99.95 wt%, Alfa Aesar, Germany) was used for investigation of the dehydration reaction.

TG-FT-IR experiments (corundum pans; heating rate: $20 \text{ K}\cdot\text{min}^{-1}$, atmosphere: nitrogen 5.0, purge gas flow rate: $40 \text{ mL}/\text{min}$) were carried out in a TG 209 *FI Iris*[®] thermobalance (NETZSCH-Gerätebau, Germany) coupled to

an FT-IR Tensor27[™] (Bruker Optics, Germany) for simultaneous analysis.

The powder X-ray diffraction was conducted on a Siemens D5000 diffractometer using $\text{CuK}\alpha_1$ radiation in a 2-theta range of 10° – 85° . Rietveld structure refinement was carried out using the GSAS program [13].

High temperature powder X-ray diffraction results were obtained by using a Stoe Stadi P diffractometer ($\text{MoK}\alpha_1$ radiation) in a 2-theta range of 10° – 60° . The samples were filled into 0.3-mm-fused silica capillaries and heated from 25 to 800°C in temperature steps of 50°C .

Scanning electron microscopy (Hitachi S-2700, Japan) was used to identify particle geometry as well as microstructures of the samples.

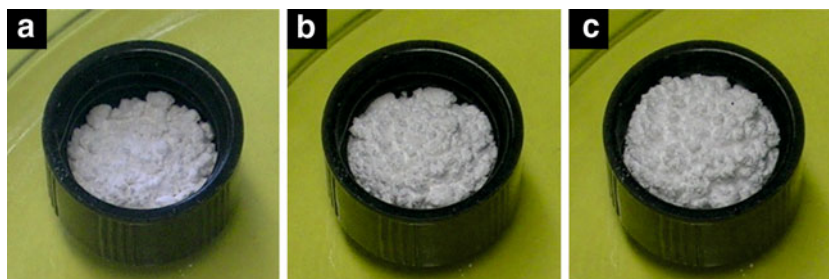
BET-experiments using nitrogen to study the specific surface area were performed using an Autosorb-1 equipment (Quantachrome, Germany).

The concentration of carbon was determined by a CHNS-Analyzer Flash EA 1112 (Thermo Electron Corporation, USA). Oxygen was measured with a TC-300 Analyzer (Leco, Germany).

Results and discussion

Following the release of the water up to 650°C , thermogravimetric investigations on commercial $\text{La}(\text{OH})_3$ showed

Fig. 3 Photographic documentation of the increase in volume during the reaction of La_2O_3 to $\text{La}(\text{OH})_3$; **a** after 1 h, **b** after 10 h, and **c** after 18 h



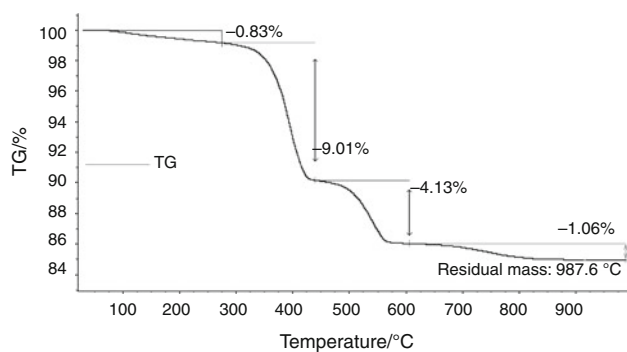


Fig. 4 TG results of $\text{La}(\text{OH})_3$, synthesized under CO_2 -free conditions

a further mass loss of 1–2% which could no longer be attributed to the release of water. With the help of TG-FT-IR measurements, the release of CO_2 (Figs. 1, 2) was

Fig. 5 Results of the Rietveld refinement of the carbonate-free $\text{La}(\text{OH})_3$; experimentally determined diffractogram (circles); calculated diffractogram (upper line); reflex positions (vertical lines); differential curve (lower line)

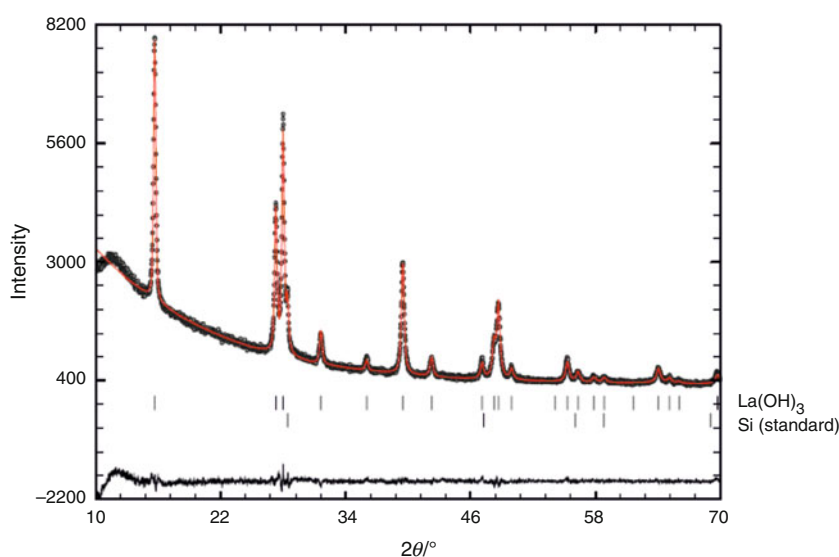
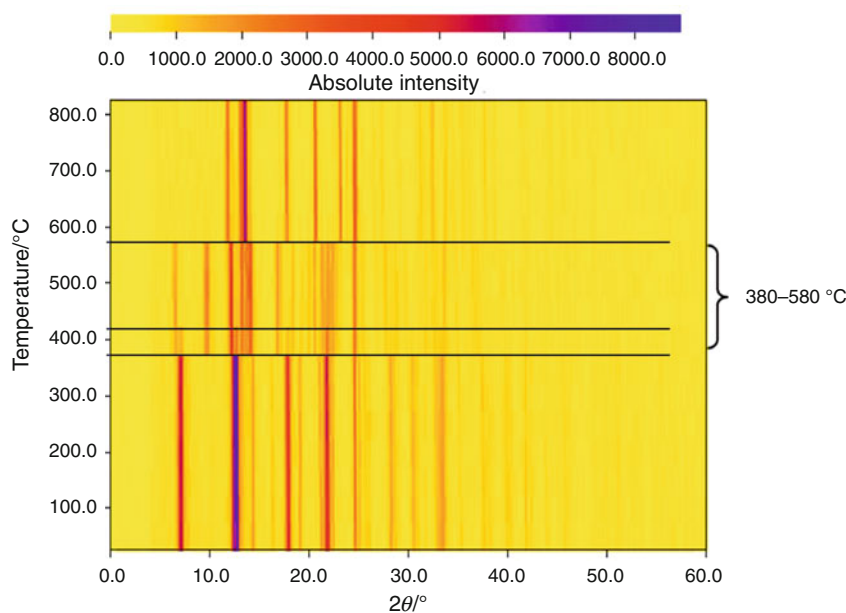


Fig. 6 Temperature-dependent X-ray diffraction pattern of $\text{La}(\text{OH})_3$



detected in the temperature range from 600 to 800 °C. Previous investigations carried out exclusively by means of thermogravimetry (i.e., not coupled for a complete TG-FT-IR system) had led Yamamoto et al. to the erroneous assumption that the mass-loss step between 600 and 850 °C [14] was caused by the release of water. As detected, $\text{La}(\text{OH})_3$ can include carbonate impurities which withstand the thermal transformation process from $\text{La}(\text{OH})_3$ to La_2O_3 at 600 °C (Fig. 1).

As a consequence, the synthesis route of carbonate-free $\text{La}(\text{OH})_3$ had to be changed in such a way as to prevent carbon dioxide access. Carbonate-free and X-ray crystalline $\text{La}(\text{OH})_3$ was obtained by an additional heating treatment (950 °C, argon atmosphere (Argon 5.0, Linde, Germany) to form La_2O_3 . For the reformation of the hydroxide, the La_2O_3 obtained was treated in a humid

argon atmosphere at 25 °C for 24 h. This reaction is accompanied by an increase in volume (~85%) which is finished after approximately 18 h (Fig. 3). The use of protective gases during synthesis and for substance storage normally serves to prevent undesired reactions with atmospheric oxygen or atmospheric humidity. In this case, however, argon was used as a protective atmosphere for the synthesis of a hydroxide, in order to prevent the $\text{La}(\text{OH})_3$ from reacting with the CO_2 content in air.

TG-FT-IR measurements of the freshly prepared $\text{La}(\text{OH})_3$ proved that the $\text{La}(\text{OH})_3$ being used for further investigations was nearly carbonate-free (Fig. 4). The residual carbonate content of approximately 0.2% (elementary analysis) is due to the fast absorption reaction of carbon dioxide from the air upon insertion into the measuring instrument. The release of CO_2 from the carbonate was further confirmed by the results of the thermogravimetric investigation, which showed a mass loss of 0.5% between 600 and 800 °C.

The results of the crystal structure determination of the $\text{La}(\text{OH})_3$ thus obtained by means of Rietveld refinement are depicted in Fig. 5. $\text{La}(\text{OH})_3$ crystallizes in a hexagonal structure with the crystal space group $P6_3/m$. The Rietveld refinement yields the lattice parameters of $a = 652.73(4)$ pm, $c = 385.47(2)$ pm, and $V = 142.23(1) \cdot 10^6$ pm³ ($R_{\text{Bragg}} = 0.026$). These values are in good agreement with the structural parameters described by Beall et al. [15] and are comparable with the values of the $\text{La}(\text{OH})_3$ samples prepared from lanthanum nitrate.

It was possible to confirm the two-step dehydration mechanism of $\text{La}(\text{OH})_3$ detected by means of thermogravimetry (Fig. 4) via temperature-dependent X-ray diffraction (HT-XRD). The results presented in Fig. 6 show the temperature range in which $\text{La}(\text{OH})_3$ (<420 °C), lanthanum hydroxide oxide (380–580 °C), and La_2O_3 (>580 °C) were detected [10]. Further the specific surface area of $\text{La}(\text{OH})_3$ (diameter of particle size detected by SEM, ~1 µm) decreases with progress of dehydration reaction. BET-measurements resulted in 18.4 m² g⁻¹ ($\text{La}(\text{OH})_3$), 8.2 m² g⁻¹ (lanthanum hydroxide oxide), and 6.6 m² g⁻¹ (La_2O_3).

Conclusions

As a result of its property of binding CO_2 from the air, $\text{La}(\text{OH})_3$ can develop impurities of the general form $\text{La}_2(\text{CO}_3)_3 \cdot x\text{H}_2\text{O}$ (lanthanum carbonate), $\text{La}_2\text{O}(\text{CO}_3)_2 \cdot x\text{H}_2\text{O}$, $\text{La}_2(\text{OH})_4 \cdot \text{CO}_3 \cdot x\text{H}_2\text{O}$ (lanthanum hydroxide carbonate), and/or $\text{La}_2\text{O}_2 \cdot \text{CO}_3 \cdot x\text{H}_2\text{O}$ (lanthanum oxide carbonate). These potential $\text{La}(\text{OH})_3$ impurities always occur in small concentrations and are also mostly amorphous and non-crystalline, and can therefore not be detected by means of X-ray analysis. By

combining thermogravimetry (TG) and Fourier Transform Infrared Spectroscopy (FT-IR), it was possible not only to fully detect and quantify these impurities but also to identify the gases released during thermal treatment. Erroneous classification or interpretation of thermoanalytical data can thus be avoided. In consequence, these results led to a change in the synthesis of $\text{La}(\text{OH})_3$, since the surrounding protective atmosphere plays a decisive role.

Acknowledgements We would like to thank Dr. Anja Neumann and M.Sc. Elena Haibel for providing sample material and helpful discussions.

References

- Barnard KR, Foger K, Turney TW, Williams RD. Lanthanum cobalt oxide oxidation catalysts derived from mixed hydroxide precursors. *J Catal.* 1990;125:265–75.
- Vishnyakov AV, Korshunova IA, Kochurikhin VE, Sal'nikova LS. Catalytic activity of rare earth oxides in flameless methane combustion. *Kinet Catal.* 2010;51:273–8.
- Sampath S, Kulkarni NK, Subramanian MS, Jayadevan NC. Effect of lanthanum, neodymium, thorium, uranium, and plutonium compounds on graphite oxidation. *Carbon.* 1988;26:129–37.
- Li SL, Zhang SX, Hu H, Zhang YH. Influence of pulse discharge plasma on composition of La_2O_3 catalyst. *Chin J Catal.* 2004;25:762–6.
- Lin CH, Campbell KD, Wang JX, Lunsford JH. Oxidative dimerization of methane over lanthanum oxide. *J Phys Chem.* 1986;90:534–7.
- Wan HL, Zhou XP, Weng WZ, Long RQ, Chao ZS, Zhang WD, Chen MS, Luo JZ, Zhou SQ. Catalytic performance, structure, surface properties and active oxygen species of the fluoride-containing rare earth (alkaline earth)-based catalysts for the oxidative coupling of methane and oxidative dehydrogenation of light alkanes. *Catal Today.* 1999;51:161–75.
- Ertl G, Knözinger H. *Handbook of heterogeneous catalysis.* Weinheim: Wiley; 1997.
- Walter D. Kinetic analysis of the transformation from lanthanum hydroxide to lanthanum oxide. *Z Anorg Allg Chem.* 2006;632:2165.
- Christensen AN. Hydrothermal preparation and low temperature magnetic properties of TbOOH , DyOOH , HoOOH , ErOOH , and YbOOH . *J Solid State Chem.* 1972;4:46–51.
- Neumann A, Walter D. The thermal transformation from lanthanum hydroxide to lanthanum hydroxide oxide. *Thermochim Acta.* 2006;445:200–4.
- Fleming P, Farrell RA, Holmes JD, Morris MA. The rapid formation of $\text{La}(\text{OH})_3$ from La_2O_3 powders on exposure to water vapor. *J Am Ceram Soc.* 2010;93:1187–94.
- Bernal S, Botana FJ, Garcia R, Rodriguez-Izquierdo JM. Thermal evolution of a sample of La_2O_3 exposed to the atmosphere. *Thermochim Acta.* 1983;66:139–45.
- Larson AC, von Dreele RB. *GSAS 1994 Version 2000.* Vol. 86. Los Alamos National Laboratory Report (LAUR); 2000.
- Yamamoto O, Takeda Y, Kanno R, Fushimi M. Thermal-decomposition and electrical-conductivity of $\text{M}(\text{OH})_3$ and MOOH ($\text{M} = \text{Y}$, Lanthanide). *Solid State Ionics.* 1985;17:107–14.
- Beall GW, Milligan WO, Wolcott HA. Structural trends in lanthanide trihydroxides. *J Inorg Nucl Chem.* 1977;39:65–70.